⌘ *Author's Choice*

THE JOURNAL OF BIOLOGICAL CHEMISTRY VOL. 285, NO. 51, pp. 40148–40162, December 17, 2010

The Dyslexia-associated KIAA0319 Protein Undergoes Proteolytic Processing with γ-Secretase-independent Intramembrane Cleavage*[S]

Received for publication, May 25, 2010, and in revised form, September 10, 2010 Published, JBC Papers in Press, October 13, 2010, DOI 10.1074/jbc.M110.145961

Antonio Velayos-Baeza, Clotilde Levecque, Kazuhiro Kobayashi[1], Zoe G. Holloway, and Anthony P. Monaco[2]

From the Wellcome Trust Centre for Human Genetics, University of Oxford, Oxford OX3 7BN, United Kingdom

The *KIAA0319* gene has been associated with reading disability in several studies. It encodes a plasma membrane protein with a large, highly glycosylated, extracellular domain. This protein is proposed to function in adhesion and attachment and thought to play an important role during neuronal migration in the developing brain. We have previously proposed that endocytosis of this protein could constitute an important mechanism to regulate its function. Here we show that KIAA0319 undergoes ectodomain shedding and intramembrane cleavage. At least five different cleavage events occur, four in the extracellular domain and one within the transmembrane domain. The ectodomain shedding processing cleaves the extracellular domain, generating several small fragments, including the N-terminal region with the Cys-rich MANEC domain. It is possible that these fragments are released to the extracellular medium and trigger cellular responses. The intramembrane cleavage releases the intracellular domain from its membrane attachment. Our results suggest that this cleavage event is not carried out by γ-secretase, the enzyme complex involved in similar processing in many other type I proteins. The soluble cytoplasmic domain of KIAA0319 is able to translocate to the nucleus, accumulating in nucleoli after overexpression. This fragment has an unknown role, although it could be involved in regulation of gene expression. The absence of DNA-interacting motifs indicates that such a function would most probably be mediated through interaction with other proteins, not by direct DNA binding. These results suggest that KIAA0319 not only has a direct role in neuronal migration but may also have additional signaling functions.

Dyslexia, or reading disability, is a genetically complex, common neurobehavioral disorder affecting between 5 and 10% of school children (1). A number of candidate genes for dyslexia have been identified (1–3). The available data from functional studies on the candidate genes *ROBO1*, *DYX1C1*, *DCDC2*, and *KIAA0319* and their encoded proteins support the hypothesis that impaired neuronal migration is a cellular neurobiological antecedent to dyslexia (4, 5). ROBO1 belongs to a family of proteins with important roles in neuronal development (6, 7). RNA interference experiments *in utero* have shown that knockdown of the expression of the *DYX1C1*, *DCDC2*, and *KIAA0319* rat homologous genes impairs neuronal migration in developing neocortex (5). These genes are also expressed in mature neurons, suggesting that they may be involved in other processes apart from neuronal migration.

Association of specific *KIAA0319* alleles with dyslexia seems to be related to a reduction in gene expression from the "risk haplotype" (8). A recent study of this haplotype has found several single-nucleotide polymorphisms in the promoter region of *KIAA0319* showing strong association with multiple reading disability traits; a putative binding site for the transcriptional silencer OCT-1 has been identified in the dyslexia-associated allele of one of these polymorphisms (9). Expression knockdown in rat disrupts neuronal migration in the developing cerebral cortex and causes a marked change in the normal morphology of migrating neurons (8). After embryonic expression knockdown, brain analysis of postnatal rats revealed neurocortical malformations, in particular periventricular heterotopias, and also hypertrophy of apical dendrites; these effects are rescued by overexpression of the human *KIAA0319* gene (10).

Human *KIAA0319* has several alternative splicing variants, with variant A being the main form (11). It encodes a highly glycosylated, dimeric, type I plasma membrane protein that, in its luminal/extracellular region, contains a MANEC[3] (motif at the N terminus with eight cysteines) domain, five polycystic kidney disease (PKD) domains and a Cys-rich domain (which we refer to as "C6 domain") reminiscent of EGF-like motifs (12). The MANEC domain, formerly called MANSC (13), comprises eight conserved cysteines, is found in the N termi-

* This work was supported by the Wellcome Trust (076566/Z/05/Z; 075491/Z/04).

⌘ *Author's Choice*—Final version full access.

[S] The on-line version of this article (available at http://www.jbc.org) contains supplemental Table 1 and Figs. 1 and 2.

[1] Present address: Division of Molecular Brain Science and Neurology, Kobe University Graduate School of Medicine, Japan.

[2] To whom correspondence should be addressed: Wellcome Trust Centre for Human Genetics, University of Oxford, Roosevelt Dr., Oxford OX3 7BN, UK. Tel.: 44-1865-287502; Fax: 44-1865-287650; E-mail: anthony.monaco@well.ox.ac.uk.

[3] The abbreviations used are: MANEC, motif at N terminus with eight cysteines; ADAM, A disintegrin and metalloprotease; APP, amyloid precursor protein; BIM, bisindolylmaleimide I; EGFP, enhanced green fluorescent protein; GV, GAL4-VP16; HAI-1, hepatocyte growth factor activator inhibitor type 1; ICD, intracellular domain; I-CLiP, intramembrane-cleaving protease; IF, immunofluorescence; KCt, KIAA0319 cytoplasmic domain; KCT48, KIAA0319 C-terminal fragment of ~48 kDa; KNT12, KIAA0319 N-terminal fragment of ~12 kDa; MEF, mouse embryonic fibroblast; PKD, polycystic kidney disease; PMA, phorbol 12-myristate 13-acetate; PS, presenilin; RIP, regulated intramembrane proteolysis; SP, signal peptide; TM, transmembrane; TM-Ct domain, TM plus cytoplasmic domain; Bis-Tris, 2-[bis(2-hydroxyethyl)amino]-2-(hydroxymethyl)propane-1,3-diol.

nus of higher multicellular animal membrane and extracellular proteins, and may play a role in the formation of protein complexes involving various protease activators and inhibitors (see NCBI CDD entry smart00765 (14)). PKD domains have been implicated in cell adhesion or cell-cell interactions (15). The presence of five PKD domains in the ectodomain region of KIAA0319 suggests that this protein could mediate adhesion between neurons and glial fibers during neuronal migration (8). Moreover, the detection of a secreted, non-membrane, minor isoform points toward a putative role in signaling (12).

We have recently reported that KIAA0319 undergoes endocytosis from the plasma membrane through a clathrin-mediated pathway, a process that controls the levels of protein at the cell surface and, thus, may be involved in regulating the role of KIAA0319 in neuronal migration (16). Cell-cell and cell-extracellular matrix interactions can be modulated by several mechanisms. Proteolytic cleavage of the extracellular domain has been described in many adhesion proteins (17, 18), where it seems to play an important role in the regulation of such interactions. This proteolytic release of extracellular domains from their membrane-bound precursor is known as ectodomain shedding (19) and is mostly carried out by metalloproteinases, in particular by members of the "a desintegrin and metalloprotease" (ADAM) family (20–22) and also by matrix metalloproteinases (23). Ectodomain shedding affects a large group of transmembrane proteins, and therefore, its functional outcome depends on the particular protein considered (19). Activation of membrane-anchored growth factors or cytokines, activation and inactivation of receptors, and regulation of cell adhesion, to mention a few, depends upon this process (20, 22, 24–26). Ectodomain shedding is usually followed by a different proteolytic mechanism involving cleavage within the plane of the membrane, which has been denominated regulated intramembrane proteolysis (RIP) (27). This process releases the cytoplasmic or luminal/extracellular domains from the membrane and allows them to translocate to a new location where they can elicit a biological response (28). RIP is mediated by the so-called Intramembrane-cleaving proteases (I-CLiPs), including aspartyl proteases (γ-secretase and signal peptide peptidase), metalloproteases (site 2 protease), and serine proteases (romboids) (29–31). γ-Secretase is the most studied of the I-CLiPs, mainly due to its participation in the processing of the amyloid precursor protein (APP) and, therefore, in the biology of Alzheimer disease (32). It is a complex formed by four hydrophobic proteins, with presenilin as its catalytic core (33, 34), and is usually involved in cleavage of type I single-TM proteins (30). A very well characterized example of RIP is the activation of the Notch signaling pathway; the resulting intracellular domain (ICD) translocates to the nucleus where it activates the expression of different target genes (35). Similarly, some of the intracellular cleavage products that are generated from different proteins after RIP function as signaling molecules, but others may be intermediates destined for degradation (36, 37).

We report here the finding that KIAA0319 undergoes ectodomain shedding and RIP. As a result, N- and C-terminal fragments are released from the membrane into the extracellular medium and the cytoplasm, respectively. We show that the released cytoplasmic domain can translocate to the nucleus and, when overexpressed, co-localizes with nucleoli markers. Interestingly, RIP of KIAA0319 seems to be γ-secretase-independent. These processes could not only be involved in regulating the role of KIAA0319 in adhesion but also in other functions. We have previously suggested a putative role of a secreted isoform of KIAA0319 in signaling (12). The present study indicates the main isoform, the full-length transmembrane protein, could also have signaling functions, possibly distinct from those of the secreted isoform.

EXPERIMENTAL PROCEDURES

Plasmids—Cloning of the human *KIAA0319* gene and its mouse homologue *D130043K22Rik* has been described previously (11). Standard PCR and molecular cloning techniques were used to generate the mammalian expression plasmids listed in supplemental Table 1. Primer sequences and cloning conditions are available upon request. A graphic representation of these constructs is shown in Figs. 1, 6*A*, and 8*A*. Positive control plasmids for luciferase assays pSG5-Gal4-VP16 and pSG5-C99Δ31C-Gal4-VP16 were kindly provided by Prof. DeStrooper. The Gal4-VP16 sequence from pSG5-Gal4-VP16 was PCR-amplified with primers GV-F1 (5′-CTTAAGGTGCACA**ATGAAGCTTTCTAGAGCGCGC***AAGCTTCTGTCTTCTATCGAACAAG*-3′) and GV-R1 (5′-GATATC**TCAACCGGTTTCGAA***ACCGTACTCGTCAATTCC*-3′) (specific Gal4-VP16 sequence are shown in italics; extra coding sequence is shown in bold) to introduce new restriction sites, and cloned into pGEM-T vector (Promega). An AflII-AgeI fragment was then subcloned into pcDNA4-TO-mycHisA vector to obtain pcD-GVm (see Fig. 8*A*). This sequence was then exchanged with the C-terminal myc-His tag in plasmids pcD4KHAm and pcD4KHAmd3-14b (#3 and 15 in Fig. 1 and supplemental Table 1) using the single sites XbaI (tag) and XmnI (plasmid backbone) to obtain, respectively, pcD4KHAGV and pcDKHAd3–14bGV (supplemental Table 1 (#29–30) and Fig. 8*A*).

Reagents—Specific antiserum R2 against the ectodomain of human KIAA0319 protein has been previously described (12). Custom polyclonal rabbit antiserum R7 against the cytosolic domain of KIAA0319 was obtained from Eurogentec Ltd after immunization with peptides (G+H) (residues 1017–1031 (C+ELRPKYGIKHRSTEH) and 1041–1055 (C+EFESDQDTLFSRERM)) of the mouse KIAA0319 protein; peptides G and H are 100 and 80% conserved in the human KIAA0319 protein, respectively). Mouse monoclonal antibodies used as subnuclear markers for nucleoli (anti-B23), Cajal bodies (anti-coilin), and nuclear speckles (anti-sc-35) were from Sigma. Other primary antibodies were, mouse monoclonal 9E10 anti-myc, chicken anti-HA (Abcam), mouse monoclonal anti-HA, and rabbit polyclonal anti-HA (Sigma). Secondary antibodies were Alexa-Fluor 488- or 594-conjugated goat anti-mouse, anti-rabbit, or anti-chicken (Molecular Probes) for immunofluorescence (IF) and goat anti-mouse or anti-rabbit IgG-HRP (Bio-Rad) for Western blotting. Phorbol 12-myristate

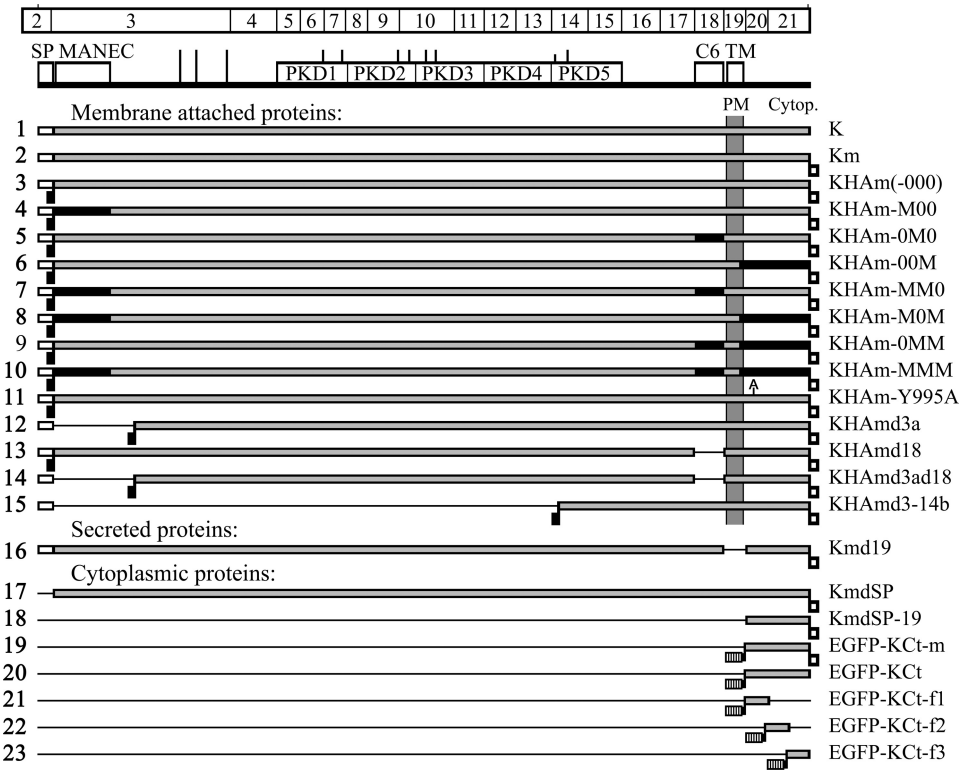

FIGURE 1. **Schematic representation of human KIAA0319 constructs.** Schemes of the *KIAA0319* cDNA (numbers indicate coding exons) and its encoded protein are shown (*top*) (12). KIAA0319 protein domains are: signal peptide (*SP*), MANEC domain, PKD (*1–5*) domains, C6 domain, and TM domain (see Introduction for more details). *Vertical lines* represent *N*-glycosylation consensus sites (glycosylation is not predicted in the first site in PKD5 (*short line*)). The different constructs used in this work appear *numbered*, grouped according to the expected localization of the encoded proteins (membrane-attached, secreted, or cytoplasmic). The name of each protein is shown on the *right*; other details are described in supplemental Table 1. Non-modified regions appear as a *gray bar*, except the SP, which is shown as a *white bar*. Deleted regions of the protein are represented as a *line*. Mutated Cys-rich domains are indicated as a *black bar*. In construct #11, *A* indicates Y995A mutation. HA, EGFP, and myc+His tags are shown as *filled*, *semi-filled*, and *open areas*, respectively, just *below each construct*. Vector backbones are pcDNA4-TO-mycHis (#1 to 18) and pEGFP-C1 (#19–23). *PM*, plasma membrane; *Cytop.*, cytoplasm.

13-acetate (PMA), bisindolylmaleimide I (BIM), and InSolution γ-secretase Inhibitor IX (or DAPT) were obtained from Calbiochem. L-685458 was obtained from Tocris Bioscience.

Cells, Cell Culture, Cell Transfection, and Standard Analyses—Human embryonic kidney 293T cells were used for most experiments. Mouse embryonic fibroblast (MEF) stable cell lines obtained from WT and from γ-secretase-deficient $PS1^{-/-}$, $PS2^{-/-}$ double knock-out (KO) mice (38, 39) were kindly provided by Prof. DeStrooper. Cells were grown in Dulbecco's modified Eagle's medium (Sigma) supplemented with 10% (v/v) fetal bovine serum (FBS), 2 mM L-glutamine, and 100 units/ml penicillin/streptomycin at 37 °C with 5% CO_2. For transfection, MEFs and 293T cells were seeded at 25,000 and 50,000 cells/cm^2, respectively, and transfected the following day (200–500 ng of plasmid DNA/cm^2) using Lipofectamine LTX and PLUS reagent (Invitrogen) for MEFs and GeneJuice (Novagen) or 25-kDa-branched polyethyleneimine (Aldrich) (40) for 293T. Cells were processed 36–48 h post-transfection. For drug treatments, medium was removed 24–30 h after transfection and new medium containing DMSO (2.5 μl/ml), PMA (1 μM), BIM (2 μM), inhibitor IX (2 μM), or L-685458 (5 μM) was added as needed. Cells were incubated for an additional 16–24-h period before being processed. IF microscopy, protein preparation, Western blotting, and analysis of glycosylation were carried out essentially as previously described (12). NuPAGE Novex 10, 12, and 4–12% Bis-Tris gels (Invitrogen) were used. For the analysis of conditioned medium from 293T cells, the FBS concentration was usually reduced to 1% when the medium was changed. Conditioned medium was collected and centrifuged at 6000 × *g* for 10 min at 4 °C, and about 30 μl were loaded per lane.

Luciferase Assays—293T, WT MEF, and KO MEF cells were seeded in 24-well plates and transfected with 200 ng of pFR-Luc plasmid (Promega) DNA and 200 ng of inducer plasmid DNA: pSG5-Gal4-VP16, pcD-GVm, pSG5-C99Δ31C-Gal4-VP16, pcD4KHAGV, or pcDKHAd3–14bGV (supplemental Table 1 and Fig. 8*A*). Cells were incubated with DMSO or the γ-secretase inhibitor L-685458 as mentioned above. The dual luciferase reporter assay system (Promega) was used following the manufacturer's instructions. Cells were lysed in a final volume of 100 μl of passive lysis buffer. The luminescence of 20 μl of lysis product was measured using a microplate luminometer (Luminoskan Ascent, Thermo Fisher Scientific). All experiments were performed in triplicate. Data were analyzed and graphed using Prism 5 (GraphPad Software).

RESULTS

KIAA0319 Undergoes Proteolytic Cleavage—We have previously shown that KIAA0319 is a plasma membrane protein, highly glycosylated, and most probably with a homodimeric conformation (12). Its predicted size without any modifica-

tion is 116 kDa. When overexpressed in mammalian cells, it is normally detected as four bands corresponding to monomeric/dimeric and partially/fully glycosylated forms, with an apparent size of around 150, 200, 300, and 400 kDa. Separation of the proteins by SDS-PAGE on gels of higher concentration (10, 12, 4–12%) than those initially used (3–8%) and detection of KIAA0319 with antibodies recognizing the C terminus of the protein revealed fragments smaller than expected. After overexpression of a C-terminal myc+His-tagged full-length construct in 293T cells, blotting of lysates with specific antiserum R7, recognizing the cytosolic domain of KIAA0319, detected the full-length protein fragments but also several other smaller bands with apparent sizes of around 48, 26, and 20 kDa (Fig. 2*A*, *left panel*, *first lane* (*Km*)); the band detected above the 35-kDa marker corresponds to the dimeric form of the 20-kDa fragment (see Fig. 3 for more details). None of these fragments was detected when non-membrane KIAA0319 proteins were overexpressed; a cytosolic protein construct without the signal peptide (*second lane* (*KmdSP*)) was only detected as two large bands (monomeric/dimeric forms), whereas a secreted protein lacking the TM domain (*third lane* (*Kmd19*)) was detected as two or three large fragments corresponding to differently glycosylated monomeric forms. All these newly detected C-terminal fragments are bigger than the cytosolic domain of the protein (*fourth lane* (*KmdSP-19*)), suggesting that they are plasma membrane-attached forms. Specific antiserum R2 (Fig. 2*A*, *right panel*), which recognizes an epitope at the PKD2 domain, only detected the full-length fragments of the overexpressed proteins, except for KmdSP-19 (*fourth lane*), which lacks this region.

According to their apparent size, the 20- and 26-kDa fragments are probably generated after cleavage around the C6 domain. The 48-kDa fragment could be either the result of cleavage around the C-terminal end of the PKD domains region or the dimeric form of the 26-kDa fragment. To check this possibility, we took advantage of the fact that the PKD region of KIAA0319 is *N*-glycosylated. After treatment with peptide *N*-glycosidase F, the 48-kDa band had a clear size shift (Fig. 2*B*), which confirmed that it is indeed *N*-glycosylated. As the last *N*-glycosylation site in the ectodomain of the KIAA0319 protein is Asn733 (11), in the PKD5 domain, the cleavage event that generates this fragment must occur N-terminal to this position.

We checked that these C-terminal fragments were not an artifact due to the C-terminal tagging of the protein. The same fragments were detected in lysates from cells overexpressing the human KIAA0319 untagged protein (Fig. 2*C*, *first lane* (*K*)) but with smaller sizes due to the absence of the C-terminal tag. Similarly, the same band pattern was detected in lysates from cells overexpressing the mouse (myc+His-tagged) protein (Fig. 2*C*, *third lane* (*mKm*)), the bands being slightly smaller than for the human tagged protein (*second lane* (*Km*)).

To detect the most N-terminal region of the ectodomain of KIAA0319, we prepared new expression constructs to introduce an HA tag just after the signal peptide sequence, before the MANEC domain (see Fig. 1). This modification had no effect on the expression or localization of the protein (data not shown). The same C-terminal band pattern was obtained with both the N-terminal untagged construct (*Km*) (Fig. 2*D*, *left panel*, *first lane*) and the new N-terminal-HA/C-terminal-myc+His-tagged construct (*KHAm*) (*second lane*); only the full-length bands of this new protein were detected in lysates with an anti-HA antibody (*middle panel*, *second lane*). We checked the conditioned media for HA-tagged fragments, and a band of about 12 kDa was detected in medium from cells overexpressing KHAm protein (Fig. 2*D*, *right panel*, *second lane*). This result indicated that another cleavage event, different from those described above, was needed to generate this small fragment and, according to its size, such an event will occur shortly C-terminal of the MANEC domain.

The above data suggest the KIAA0319 protein undergoes ectodomain shedding. This process can be stimulated by a number of factors (20), phorbol esters being among the most commonly used (19). We checked if treatment of transfected cells with PMA had any effect on the band pattern detected. A new C-terminal band of about 18 kDa appeared in the lysates of PMA-treated cells over-expressing the KHAm protein (Fig. 2*E*). The specific cleavage point at which this fragment originates has not been determined; however, its size, slightly larger than KmdSP-19 (Fig. 2*A*), was consistent with the RIP intramembrane cleavage events that usually follow ectodomain shedding in many proteins. The detected cleavage fragments were named as KIAA0319 C-terminal fragment of ~48 (KCT48), 26 (KCT26), 20 (KCT20), and 18 kDa (KCT18) (all of these including the myc+His tag, ~3.4 kDa), and KIAA0319 N-terminal fragment of ~12 kDa (KNT12) (including the HA-tag, ~1.3 kDa).

In other proteins undergoing ectodomain shedding and RIP, deletion constructs mimicking some forms of the cleaved proteins present an up-regulated RIP. We tested if a similar effect occurred in the processing of a deletion KIAA0319 construct where most of the region N-terminal to the last *N*-glycosylation site had been removed. The deletion protein KHAmd3-14b, where residues 23–721 have been removed, has an expected size of 46.4 kDa (supplemental Table 1), and its apparent size is similar to that of KCT48 (Fig. 2*F*, *arrowhead*; higher bands, marked by *asterisks*, correspond to multimers of this protein). Fragments KCT26 and KCT20 were as in the full-length KIAA0319 protein, but KCT18 was now detected without PMA induction. These results suggest that RIP in KIAA0319 is enhanced when the ectodomain fragment removed by cleavage event 2 is not present.

We demonstrated that the stimulation of KIAA0319 cleavage by PMA was due to its effect as an activator of protein kinase C (PKC) activity. Treatment of transfected cells with the PKC inhibitor BIM had no effect on the band pattern from lysates of non-PMA-treated cells (Fig. 2*G*, *left panel*; compare the *first* and *second lanes*) but completely inhibited the stimulation effect of PMA in BIM+PMA-treated cells (compare the *third* and *fourth lanes*). The same effect was detected in conditioned media (Fig. 2*G*, *right panel*); BIM inhibited the clear effect of PMA, consisting not only in a much stronger signal from the 12 kDa

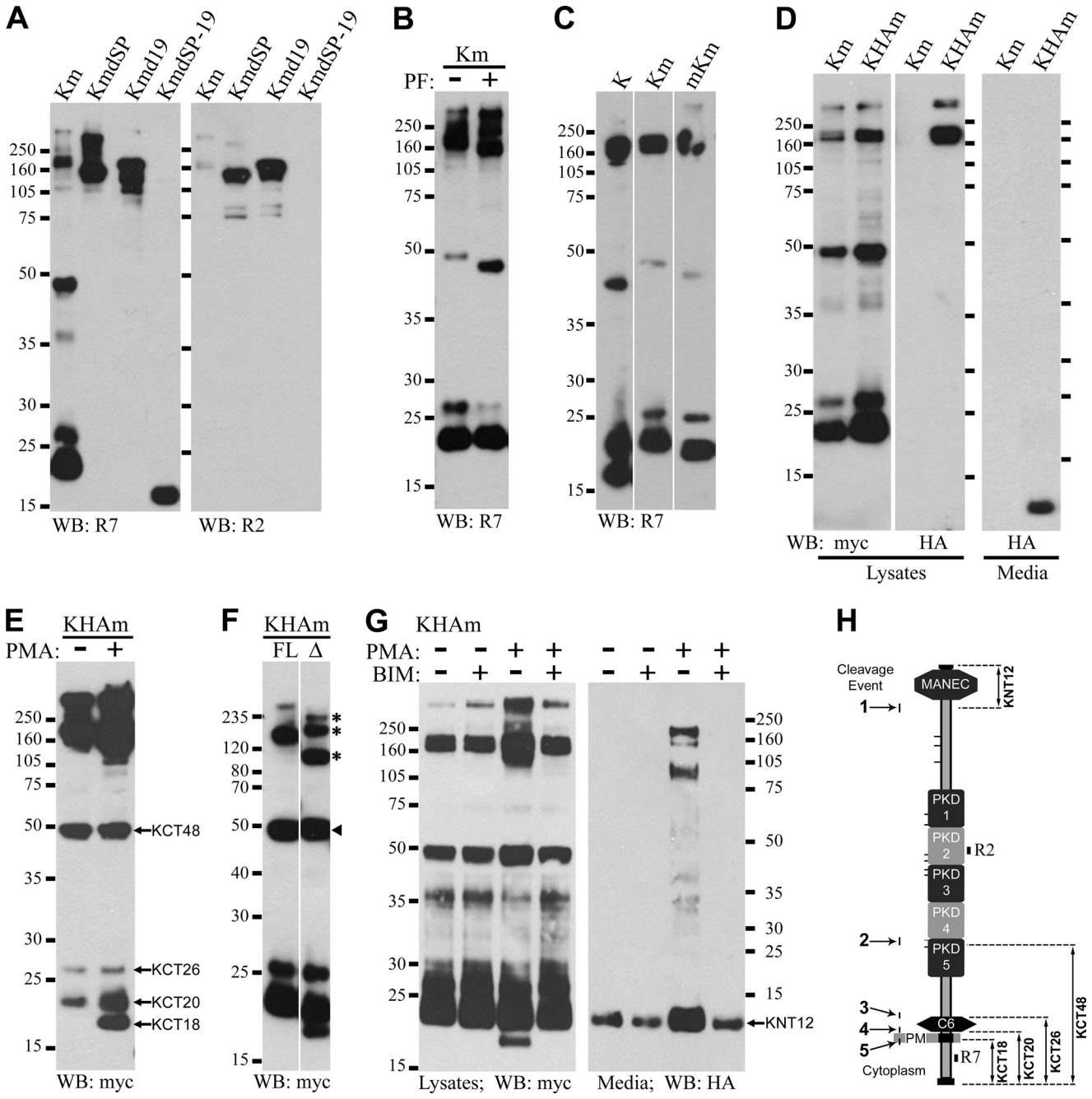

FIGURE 2. **Detection and analysis of proteolytic processing in the KIAA0319 protein.** 293T cells were transiently transfected with different KIAA0319 plasmids (see Fig. 1 and supplemental Table 1), and cell lysates or media were analyzed by Western blotting (*WB*) as indicated. *A*, several C-terminal fragments originated after ectodomain shedding were detected with specific antiserum R7 from the full-length protein (*Km*) but not from non-membrane proteins, whereas antiserum R2 only detects the non-cleaved proteins. *B*, shown is analysis of glycosylation in C-terminal fragments by treatment with peptide *N*-glycosidase F (*PF*). *C*, ectodomain shedding in differently tagged human and mouse proteins is shown. *D*, introduction of N-terminal HA tag does not affect C-terminal cleavage and allows detection of cleaved fragments in conditioned medium. *E*, PMA induces ectodomain shedding and allows detection of an extra *K*IAA0319 C-terminal fragment (*KCT*); the different fragments are indicated according to their apparent size. *F*, C-terminal cleavage is up-regulated in the deletion protein KHAmd3-14b (Δ) compared with the full-length (*FL*) KIAA0319, with the KCT18 band clearly detectable without PMA-induction. In *lane* Δ: *arrowhead*, non-cleaved deletion protein, similar to KCT48; *asterisks*, multimers of deletion protein. *G*, PMA induction is inhibited by the protein kinase C inhibitor BIM. *H*, shown is a schematic representation of the proteolytic processing of KIAA0319. The approximate location of the different cleavage events detected and the fragments originated from each of these events are shown. Protein domains, *N*-glycosylation sites (*short horizontal lines*) and epitopes recognized by the R2 and R7 specific antisera are represented (see also Fig. 1). *PM*, plasma membrane. KCT18, KIAA0319 C-terminal fragment of about 18 kDa. N-terminal HA tag and C-terminal myc-His tags are represented as *dark rectangles* and included in the size estimation of the cleavage fragments.

band but also in the detection of several high molecular weight bands most probably corresponding to N-terminal fragments originated from any of the other cleavage sites closer to the TM domain. Thus, at least five cleavage events occur during the ectodomain shedding/RIP of KIAA0319. A schematic representation is presented in Fig. 2*H*. Event 1 results in generation of KNT12; events 2–5 generate KCT48, KCT26, KCT20, and KCT18, respectively.

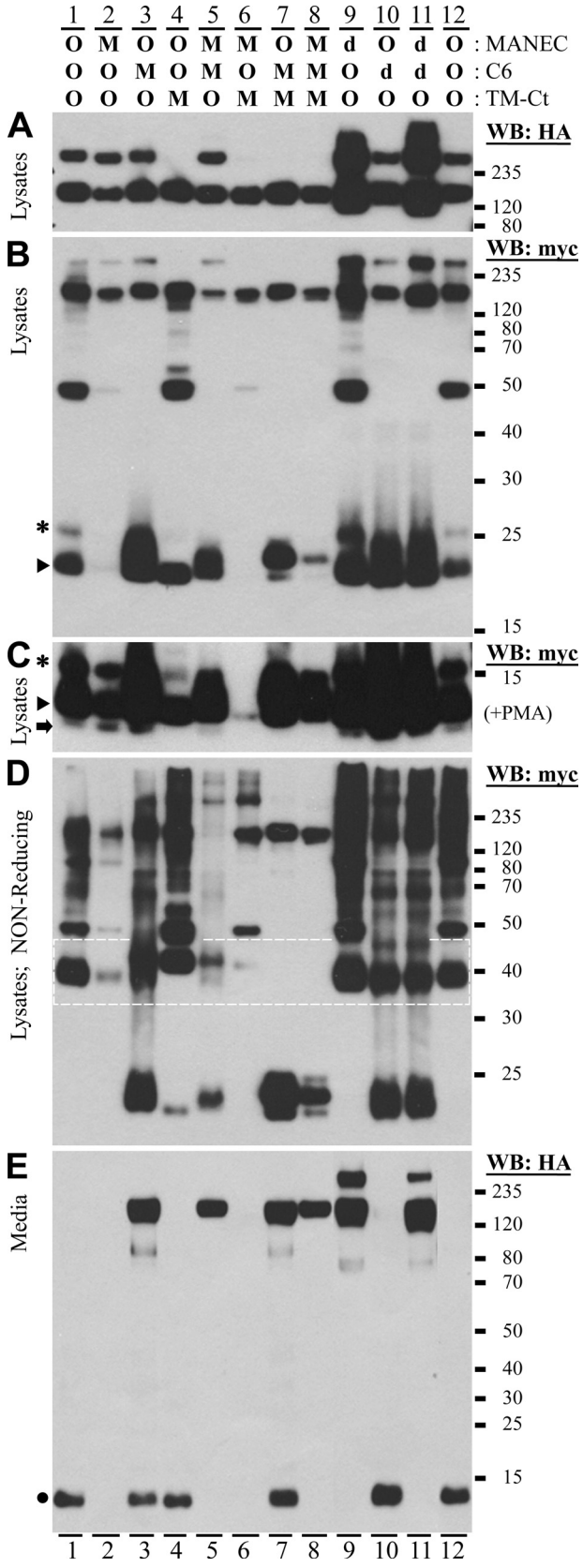

FIGURE 3. **Effect of alteration of Cys-rich domains in the cleavage of KIAA0319.** 293T cells were transiently transfected with constructs encoding KIAA0319 proteins with their MANEC, C6, and TM-Ct domains unmodified (*O*), deleted (*d*), or all-Cys residues mutated (*M*). Lysates and conditioned media were analyzed by Western blotting (*WB*) under reducing conditions, except in *D*, as indicated. *A*, detection of HA-tagged fragments in cell lysates is shown; only the bands shown were detected in the blot. *B*, detection of myc-tagged fragments in cell lysates is shown. *C*, procedures were the same as in *B* but after PMA induction; only short fragments are shown. *D*, procedures were the same as in *B* but using non-reducing conditions; the *white dashed box* indicates the dimeric forms of the KCT20 fragments. *E*, HA-tagged fragments were detected in conditioned media. Some cleavage fragments are indicated: *asterisk*, KCT26; *arrowhead*, KCT20; *arrow*, KCT18; *circle*, KNT12.

Please note that numbering of the cleavage events is not an indication of the order in which these events occur.

Integrity of the Cys-rich Domains Is Needed for Proper Cleavage of KIAA0319—The cleavage sites detected in KIAA0319, except for site 2, seemed to occur in or around the different Cys-rich domains (MANEC, C6, and TM). We used constructs encoding KIAA0319 proteins altered in these domains to investigate the role they may have in the ectodomain shedding of this protein. We have previously described a number of constructs with different combinations of domains where all the Cys residues had been mutated (M) as well as those where the MANEC and/or the C6 domains were deleted (d3a, d18, d3ad18) (12). We modified them to introduce an N-terminal HA tag as described above and used them to transfect 293T cells; lysates and conditioned media were then analyzed (Fig. 3). Western blotting with anti-HA antibody only detected the full-length fragments in cell lysates (Fig. 3*A*). As described before (12), the dimeric forms of KIAA0319 that typically persist in reducing conditions disappear in those constructs where the Cys residues of the TM-Ct domain (transmembrane plus cytoplasmic domain) are mutated (*lanes 4*, *6*, *7*, and *8*). We used anti-myc antibody to detect the C-terminal fragments (Fig. 3*B*). The full-length fragments were detected as with anti-HA antibody. The C-terminal cleavage fragments showed very clear differences between constructs. Mutation of the MANEC domain alone (*lane 2*) seemed to greatly impair the generation of cleavage fragments. Mutation of the C6 domain alone (*lane 3*) prevented the formation of the KCT48 fragment and also had an effect in the smaller fragments, which presented a very strong signal. An identical effect, especially regarding the KCT48 fragment, was obtained with single mutants of any of the six Cys residues of the C6 domain (data not shown). However, mutation of the TM-Ct domain alone (*lane 4*) did not seem to have any major effect, although KCT26 was slightly reduced when compared with the non-mutated construct (*lanes 1* and *12*). Deletion of the C6 domain (*lanes 10* and *11*) seemed to have the same effects as its mutation. However, when the MANEC domain alone was deleted (*lane 9*) there was no difference with the unmodified constructs (*lanes 1* and *12*). These results suggested that the effects detected in the MANEC domain mutant (*lane 2*) were most probably due not to the direct involvement of this domain in the C-terminal cleavage events but rather to other reasons, such as misfolding of the protein and endoplasmic reticulum retention. Alteration of the C6 domain either on its own or together with alteration of other domains not only prevented cleavage event 2, which generates KCT48, but it also seemed to induce a new cleavage event, at some point between events 3 and 4, as a new fragment with a size in be-

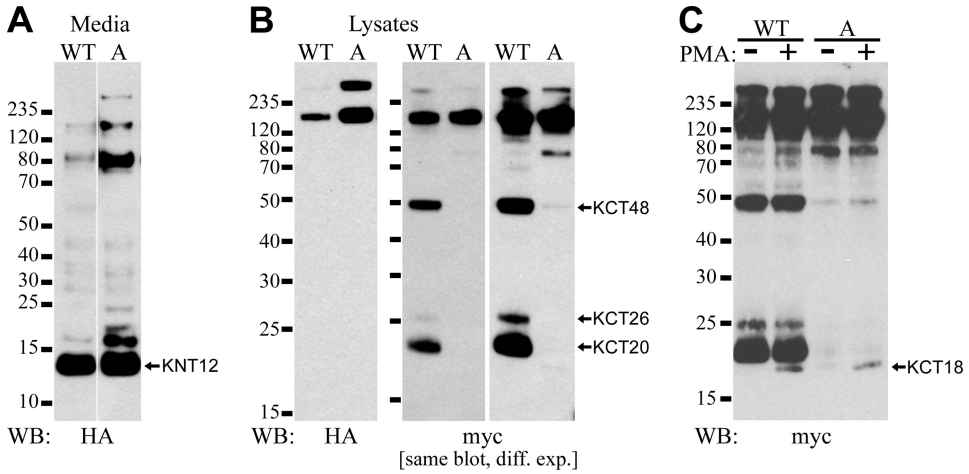

FIGURE 4. **Effect of endocytosis impairment in the cleavage of KIAA0319.** Conditioned media (*A*) and cell lysates (*B* and *C*) of 293T cells transiently overexpressing KIAA0319 full-length protein (WT) or the endocytosis-impaired mutant Y995A (*A*) (see Fig. 1) were analyzed by Western blotting (*WB*). *A*, the N-terminal cleavage fragment is detected with both wild-type and mutant constructs. *B*, the C-terminal fragments originated by ectodomain shedding are absent or highly reduced in lysates of cells transfected with the Y995A mutant. The *second panel* of myc Western blotting is a longer exposure of the blot shown on the *left* (*diff. exp.*). *C*, induction with PMA shows that the C-terminal fragment originated after intramembrane cleavage is detected with both constructs.

tween KCT26 and KCT20 was detected (see *lanes 7* and *8* in Fig. 3, (*B* and *D*)).

Identical results were obtained when cells were treated with PMA (not shown). We used these conditions to evaluate the effect that these mutations/deletions have in the generation of KCT18. This fragment seemed to be absent or greatly reduced in those constructs where the TM-Ct was mutated (Fig. 3*C*, *lanes 4*, *6*, *7*, and *8*), which suggests that at least some of the Cys residues in the TM/juxtamembrane region of the cytoplasmic domain are important for cleavage event 5 to happen.

We also checked the cell lysates in non-reducing conditions (Fig. 3*D*). The smaller fragments of 20 and 26 kDa were absent in the unmodified protein; instead, a new band of around 40-kDa appeared (*lanes 1* and *12*); this size is compatible with a dimeric form of KCT20, and these results indicate that these C-terminal cleavage fragments are most probably produced as dimers. No new band corresponding to the dimeric form of KCT26 was detected, but this can be explained by coincidence in size with the KCT48 fragments. Thus, the 48-kDa band detected in these conditions could be a mixture of monomeric KCT48 and dimeric KCT26 or just the latter, whereas KCT48 would be in dimeric form too, with a size of about 100kDa (this band is also detected). Similar results were obtained with constructs where both C6 and TM-Ct domains were unmodified (*lanes 2* and *9*). Modification of any of these two domains (*lanes 3*, *4*, *5*, *6*, *7*, *8*, *10*, and *11*) led to detection of the monomeric forms (please note that this is not apparent in *lane 6*, most probably because of the misfolding effects mentioned above). These monomeric forms were the only ones detected when both domains were modified at the same time (*lanes 7* and *8*), whereas dimeric forms were still detected with all the other constructs.

When the conditioned media were checked for HA-tagged fragments (Fig. 3*E*), it became apparent that mutation of the TM-Ct domain had no effect in the generation of these fragments (compare *lanes 1* and *4*, *2* and *6*, *3* and *7*, and *5* and *8*); this domain is not considered in the following analysis of results. The KNT12 fragment was detected with all constructs where the MANEC domain was unmodified (*lanes 1*, *3*, *4*, *7*, *10*, and *12*). High molecular weight fragments probably originated after cleavage events 3 and/or 4 were detected with all the constructs where the MANEC domain was deleted (*lanes 9* and *11*) or where the C6 domain was mutated (*lanes 3*, *5*, *7*, and *8*). In this case both KNT12 and large fragments were detected when the C6 domain was mutated but the MANEC domain was unmodified (*lanes 3* and *7*), whereas only the large fragment appeared when both domains were mutated (*lanes 5* and *8*). This suggests that integrity of the MANEC domain is necessary for cleavage event 1 to occur. Mutation of the MANEC domain alone (*lanes 2* and *6*) prevented the detection of N-terminal fragments in the conditioned medium, most probably due to misfolding and endoplasmic reticulum retention of these proteins, as described previously for the C-terminal fragments.

Internalization of KIAA0319 Is Important for C-terminal Cleavage—We have recently reported the clathrin-mediated internalization of KIAA0319 from the plasma membrane (16). Mutation of Tyr at position 995 is sufficient to inhibit KIAA0319 endocytosis. We checked the effect that this mutation had in the ectodomain shedding of this protein. Lysates and conditioned media of 293T cells transiently transfected with constructs KHAm and KHAm-Y995A were analyzed. When we checked the conditioned media of these transfected cells, the KNT12 fragment was detected in both cases (Fig. 4*A*). Larger bands were detected in particular with the internalization-impaired construct (*lane A*). These results indicate that cleavage event 1 can occur at the plasma membrane. However, an obvious reduction in the C-terminal cleavage fragments was detected with anti-myc antibody with the protein mutated at Tyr-995 (Fig. 4*B*, *right panels*, *lane A*), although the expression level of this protein was normal, as detected with anti-HA antibody (*left panel*, *lane A*). A very similar effect was detected when cells were co-transfected with the unmodified KIAA0319 full-length construct

(KHAm) and the dominant-negative mutant Rab5-S34N, which prevents internalization of KIAA0319 from the plasma membrane (data not shown). These data suggest that blocking the internalization of KIAA0319 from the plasma membrane negatively affects the ectodomain shedding of KIAA0319 that generates the C-terminal fragments KCT48, KCT26, and KCT20.

To assess if the intramembrane cleavage, generating KCT18, was also affected in the Y995A mutant, we performed a similar assay comparing PMA-induced samples with DMSO control samples (Fig. 4*C*). The control samples (*lanes WT*− and *A*−) were as described in Fig. 4*B*. After induction with PMA, KCT18 fragment was detected in the wild-type lysate (Fig. 4*C*, *lane WT*+). Interestingly, this fragment was still detected at similar levels in the mutant lysate (*lane A*+), in clear contrast with the absence/highly reduced levels of the other C-terminal fragments. These results indicate that cleavage event 5 does not require internalization from the plasma membrane.

The Cytoplasmic Domain of KIAA0319 Can Translocate to the Nucleus—Ectodomain shedding generates membrane-attached fragments that undergo RIP to produce cytoplasmic-soluble fragments that can often translocate to the nucleus. We investigated whether this was also true for KIAA0319. When we used the myc+His-tagged deletion protein KmdSP-19, overexpressed from a construct containing only exons 20 and 21 of *KIAA0319* that encode most of the cytoplasmic domain of the protein, it could indeed be detected in the nuclei of transfected cells (Fig. 5*A*). A different protein, consisting of all the deduced cytoplasmic domain of KIAA0319 (KCt) (including the CCKR sequence encoded by exon 19) with an N-terminal EGFP tag and the C-terminal myc+His tags had a much stronger nuclear localization (Fig. 5*B*). The same happened when the C-terminal tags were removed (Fig. 5*C*), which indicates that such a localization is not caused by this tagging.

To determine the region of KCt responsible for the nuclear localization, we divided the 93-residue sequence in three overlapping fragments (f1, f2, and f3; residues 980–1013, 1008–1044, and 1039–1072, respectively, of KIAA0319), as previously described for the characterization of the interaction with the μ2 subunit of the adaptor protein 2 (16). The EGFP-tagged constructs of these fragments were overexpressed in 293T cells. KCt-f1 conserved the same nuclear localization (Fig. 5*D*). KCt-f2 also had some nuclear localization, but the detected cytosolic localization was much higher than for KCt or KCt-f1 (Fig. 5*E*), and KCt-f3 presented a typical cytosolic distribution (Fig. 5*F*). These results indicate that the juxtamembrane region of KCt is responsible for its nuclear localization.

For the experiments described above we used the sequence predicted to be the cytoplasmic domain. However, in most of the reported examples of protein undergoing ectodomain shedding, the cleavage event that generates the cytosolic, soluble fragments usually happens in the transmembrane region of these proteins. We investigated the effect that the addition of residues from the TM domain of KIAA0319 to the overexpressed protein had on its subcellular localization. For this purpose we used constructs with an N-terminal HA tag and a C-terminal myc+His tag (*KHAmCt-*) (Fig. 6*A* and supplemental Table 1, #24–28). The HA tag was used for its small size to maintain conditions similar to the unmodified proteins, thus, avoiding confusion with proteins that could be expressed from any of the Met codons present in KCt. KHAmCt-980, containing only the cytoplasmic domain of KIAA0319, had nuclear localization as expected, showing accumulation in some kind of subnuclear structures rather than having an uniform distribution (Fig. 6*B*). The same happened for KHAmCt-978, containing the last two residues of the TM domain (Fig. 6*C*). The three other tested constructs (KHAmCt-973, -971, and -969; Fig. 6, *D*, *E*, and *F*, respectively) showed some nuclear localization that decreased as the number of TM-domain residues increased. The overexpressed proteins accumulated in cytosolic aggregates, an effect directly related to the increment in the number of residues from the TM domain. These results suggest that the intramembrane cleavage event that generates KCT18 probably occurs at some point after residue Phe-973 and before residue Cys-980.

We further characterized the nuclear pattern detected with constructs KHAmCt-980 (Fig. 7) and -978 (supplemental Fig. 1) by IF using several subnuclear markers to identify the structures where these proteins accumulate. KHAmCt-980 clearly co-localized with the nucleolar marker B23 (Fig. 7*A*) and showed a similar but different pattern than the Cajal bodies marker coilin (Fig. 7*B*); no co-localization was detected with the nuclear speckles marker sc-35 (Fig. 7*C*). Similar results were obtained for KHAmCt-978 (supplemental Fig. 1), but the detected structures were not as uniform as for KHAmCt-980. Cajal bodies seemed to be affected by the overexpression of the KIAA0319 protein fragments. In particular, KHAmCt-978 showed a higher degree of co-localization with coilin compared with KHAmCt-980 in some cells, whereas other transfected cells were often negative for coilin staining (supplemental Fig. 1*B*). These results suggest that the cytoplasmic domain of KIAA0319 accumulates in nucleoli and that the Cajal bodies may be disturbed by such accumulation.

KIAA0319 Undergoes γ-Secretase-independent RIP—Generation of soluble protein fragments by RIP requires the participation of I-CLiPs. γ-Secretase has been reported as the enzyme involved in most cases of type I proteins where this process has been described. We tested if this was also true for KIAA0319. Initial analyses using specific γ-secretase inhibitors DAPT and L-685458 in 293T cells transfected with KIAA0319 constructs did not show any clear effect on the levels of KCT18 fragment detected by Western blotting (data not shown). We then decided to assess the involvement of γ-secretase in KIAA0319 cleavage by a luciferase-based assay (41, 42). A GAL4-VP16 (GV) sequence was introduced as a C-terminal tag in two KIAA0319 constructs (full-length and Δ23–721) (Fig. 8*A*). These constructs were then used in co-transfection experiments with pFR-Luc, a reporter plasmid containing the firefly luciferase gene under the control of a synthetic promoter with five tandem repeats of the yeast GAL4 binding sites. Release of the GV-tagged cytosolic do-

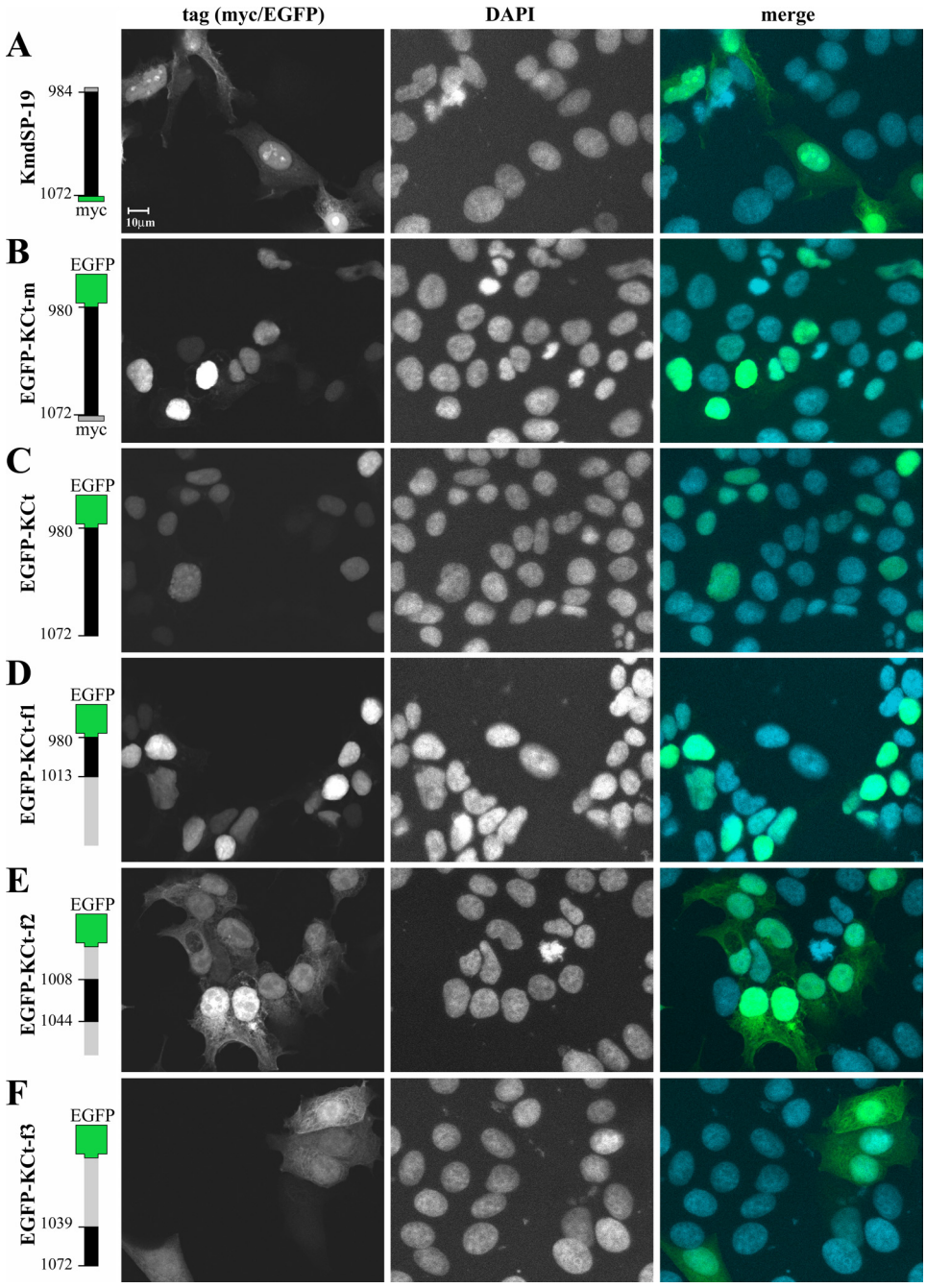

FIGURE 5. **Subcellular localization of KIAA0319 cytoplasmic domain proteins.** Several constructs overexpressing different fragments of the cytoplasmic domain of KIAA0319 were transiently transfected into 293T cells. Each of these constructs is represented on the *left of the figure*; tags and the first and last residues of the KIAA0319 protein are shown (EGFP tag not at scale). *Green* indicates the tag used for detection of these proteins by IF; *light gray* indicates regions of the cytoplasmic domain deleted in constructs shown in *panels D*, *E*, and *F*. The Myc tag was detected with anti-myc antibody. Nuclei are detected by DAPI staining. A 10-μm *bar* is shown in the *top left panel*; all panels are at the same scale.

main from the membrane-attached KIAA0319 protein after RIP will result in activation of the luciferase reporter gene. Overexpression of the soluble positive control GAL4-VP16 proteins in 293T cells, regardless of treatment with DMSO or L-685458, showed a clear increase in luciferase activity over non-transfected cells (supplemental Fig. 2*A*). As expected, when cells were transfected with construct APP-C99d31-GV, which encodes a positive control membrane-attached protein, the luciferase activity detected in control conditions was drastically reduced by treatment with the γ-secretase inhibitor (Fig. 8*B*, *APP-GV*). However, no difference was detected between control and inhibitor-treated cells after transfection with the two KIAA0319 constructs (Fig. 8*B*, *K-GV* and *KΔ-GV*). We carried out similar analyses in MEF WT cells treated with DMSO or with L-685458 and in γ-secretase-deficient MEF cells derived from PS1/PS2 double KO mice treated with DMSO. As shown for 293T cells, overexpression of positive control soluble GAL4-VP16 proteins led to activation of the reporter gene in both WT and KO cells, with no difference between control and inhibitor treatment conditions

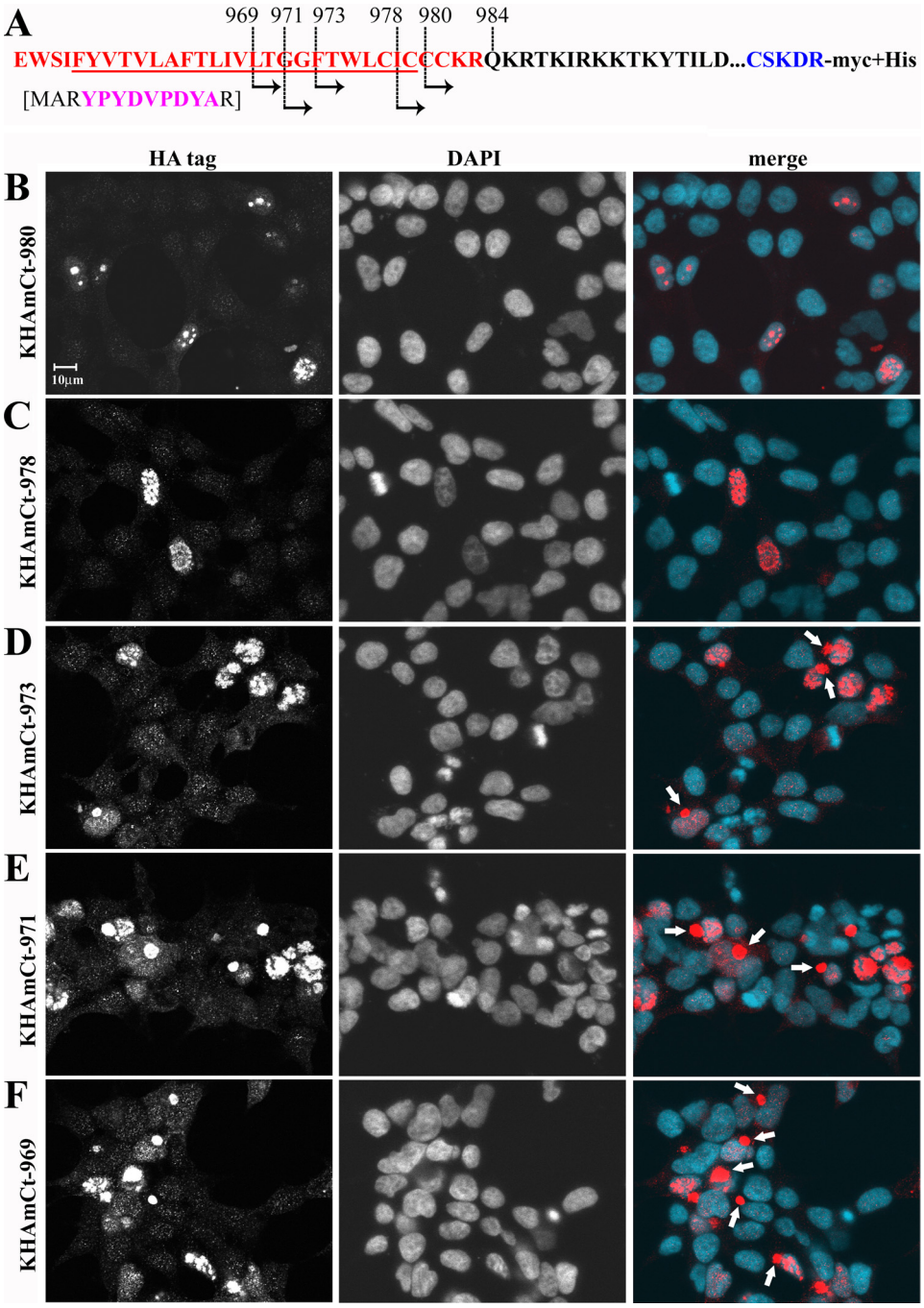

FIGURE 6. **Analysis of the effect of N-terminal elongation of the cytoplasmic domain of KIAA0319 proteins in subcellular localization.** Several constructs overexpressing the cytoplasmic domain of KIAA0319 with different numbers of residues from the TM domain, with N-terminal HA tag and C-terminal myc+His tags (KHAmCt; constructs #24–28 in supplemental Table 1), were transiently transfected into 293T cells, and the subcellular localization of the encoded proteins were analyzed by IF with rabbit anti-HA antibody. *A*, shown is a representation of the residues encoded by *KIAA0319* exons 19–21 (19 in *red*, 20 in *black*, 21 in *blue*; *dots* represent residues not shown). Predicted TM domain residues are *underlined*. N-terminal tagging, including the HA tag in *purple*, is shown in *square brackets*. The positions of the first residues from the KIAA0319 protein in these constructs are indicated. *B–F*, detection by IF of the protein encoded by the construct indicated on the *left* is shown. Cytoplasmic aggregation of these proteins is indicated in the merge panels by *white arrows*. Nuclei are detected by DAPI staining. A 10-μm *bar* is shown in the *top left panel*; all panels are at the same scale.

(supplemental Fig. 2*B*). The luciferase activity detected in control conditions in WT cells transfected with the control plasmid APP-C99d31-GV was drastically reduced in cells treated with L-685458 as expected, and the levels in KO cells were equally low (Fig. 8*C*, *APP-GV*). However, and in accordance with the results obtained with 293T cells, similar levels of luciferase activity were detected in all conditions in both WT and KO MEF cells transfected with KIAA0319 plasmids (Fig. 8*C*, *K-GV* and *KΔ-GV*). These results strongly suggest that γ-secretase is not involved in cleavage of KIAA0319.

DISCUSSION

The functional data available for the different "dyslexia-associated" proteins (encoded by the dyslexia candidate

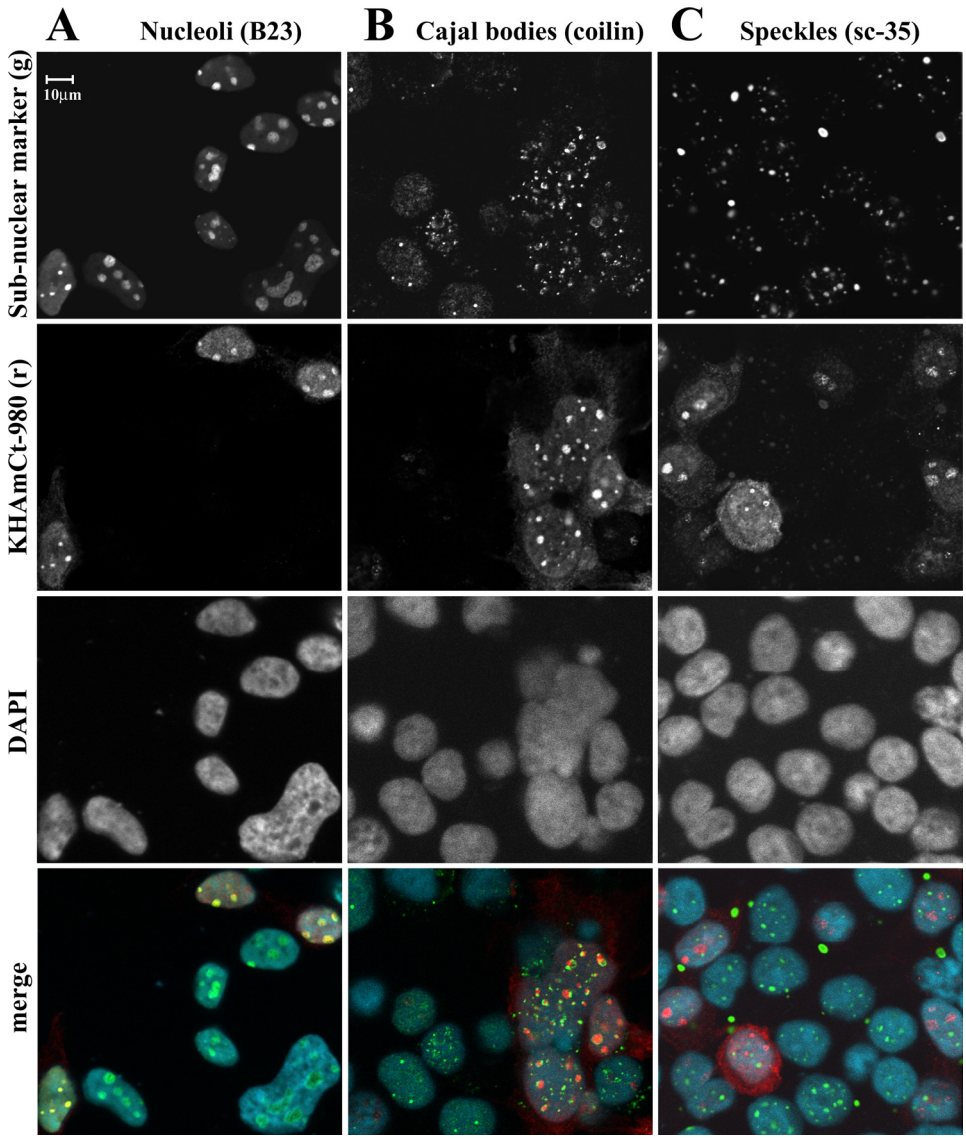

FIGURE 7. **Co-localization of KIAA0319 C-terminal fragment protein KHAmCt-980 with subnuclear markers.** KHAmCt-980 protein was overexpressed in 293T cells as described above, and its subnuclear localization was analyzed by IF with chicken anti-HA antibody (*red* in *merge panels*) and compared with that obtained with specific markers (*green* in *merge panels*) for nucleoli (B23; *A*), Cajal bodies (coilin; *B*), and speckles (sc-35; *C*). Nuclei are detected by DAPI staining. A 10-μm *bar* is shown in the *top left panel*; all panels are at the same scale.

genes) indicate that they are required for normal brain development. The participation of most of these proteins in neuronal migration has already been indicated, although this may not be their only role. Data available from homologous proteins in other organisms or from proteins sharing common domains have been used to hypothesize about the molecular mechanisms mediating their function in neuronal migration (4). In the case of KIAA0319, the PKD domains present in its extracellular region suggested that this plasma membrane protein could mediate adhesion between neurons and glial fibers (8). We show here that the main isoform of KIAA0319 with plasma membrane localization undergoes proteolytic cleavage. This processing is a new variable to take into consideration for the study and evaluation of the functional roles of KIAA0319.

We have identified at least four cleavage events in the KIAA0319 extracellular domain (ectodomain shedding). A fifth event frees the cytoplasmic domain from the membrane. The size of this fragment is consistent with cleavage at the TM domain and is assumed to represent RIP of KIAA0319. This pattern seems slightly more complex than in other proteins, where usually only one or two cleavage events occur in the ectodomain of the cleaved protein, generally located close to the membrane surface (22). Ectodomain shedding proximal to the membrane appears to be necessary for further cleavage within the membrane plane (22). KIAA0319 cleavage event 1 generates KNT12, an N-terminal fragment of about 12 kDa (all protein size estimations refer to the N-terminal HA-tagged, C-terminal myc+His-tagged protein) that contains the MANEC domain. The corresponding C-terminal fragment was not detected in our analyses or at least not as a distinctive band, most probably due to co-migration with some of the full-length fragments or because of the cleavage at the C terminus. Cleavage event 2 is located close to the

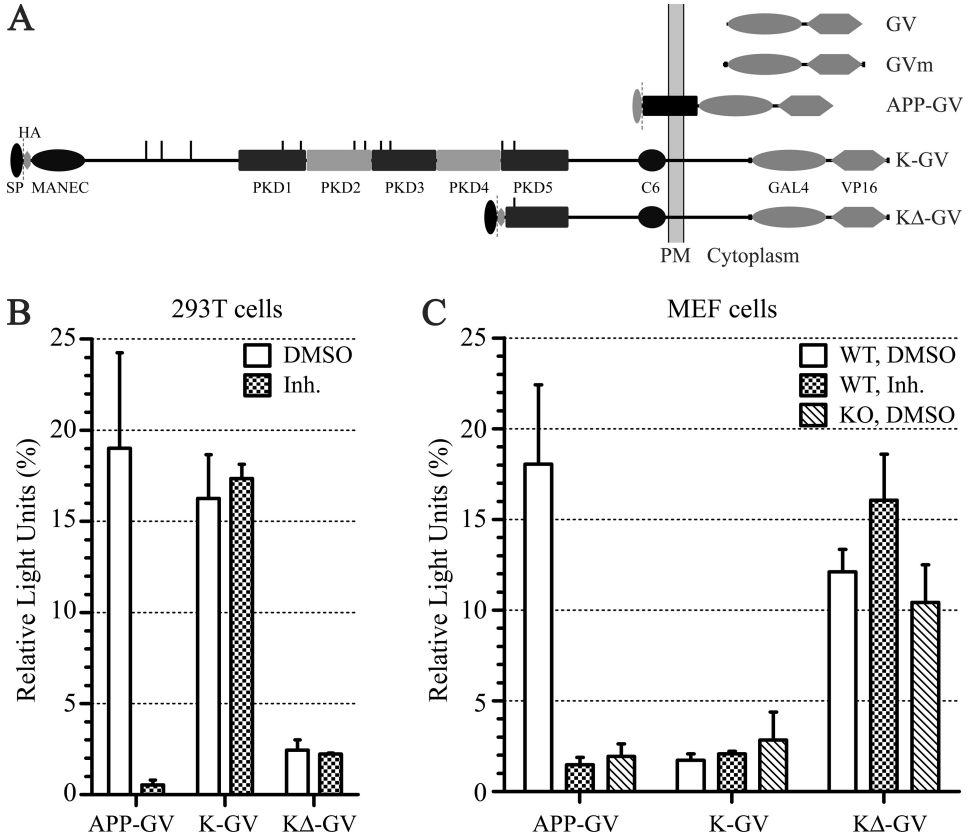

FIGURE 8. **Analysis of intramembrane cleavage of KIAA0319 by luciferase assay.** *A*, shown is a schematic representation of the proteins encoded by the constructs used in these assays (see supplemental Table 1 and "Experimental Procedures"). *B*, shown is a graphic representation of the luciferase assay results on 293T cells transfected with the indicated constructs plus pFR-Luc under control conditions (DMSO) or treated with the γ-secretase inhibitor L-685458 (*Inh.*). *C*, procedures were as in *B*, but using WT and γ-secretase-deficient PS1$^{-/-}$, PS2$^{-/-}$ double KO MEF cells. Values are normalized for the luciferase activities obtained in the same conditions with the soluble positive control pSG5-Gal4-VP16 (*GV*) and presented as means of three assays ± S.E.

junction between PKD domains 4 and 5 and generates KCT48. Events 3 and 4 are much closer to the membrane, located around the C6 domain, and their products KCT26 and KCT20, respectively, are membrane-tethered fragments with short ectodomains. Intramembrane cleavage event 5 generates KCT18, a fragment corresponding to the intracellular domain of KIAA0319, which is only detected after PMA induction in cells overexpressing the full-length protein. This fragment is easily detected without PMA induction when a deletion construct encoding a protein resembling the expected C-terminal fragment of KIAA0319 after cleavage event 2 is used. This suggests that removal of the N-terminal region of the protein activates the intramembrane cleavage, a common effect in many proteins undergoing similar processing (30).

Mutagenesis/deletion of the Cys-rich domains of KIAA0319 showed that the different cleavage events are affected by alterations of their surrounding regions, most probably due to conformational changes of the mutant protein. Although deletion of the MANEC domain has no obvious effect on cleavage (event 1 is not considered here as the cleavage site is removed in the deletion protein), mutation of the Cys residues in this domain impairs event 1. We did not find significant changes in cleavage at the ectodomain of KIAA0319 after alteration of TM-Ct domain, except for a slight reduction of KCT26; however, cleavage event 5 was clearly affected, suggesting that the Cys residues, most probably those at the junction between TM and cytoplasmic domains, are critical for RIP either because they are needed for the protein to have a particular conformation or because they form part of the cleavage site itself. Mutagenesis of the C6 domain affects, but does not impair, membrane-proximal cleavage (events 3 and 4); a new cleavage fragment, intermediate in size between KCT26 and KCT20, appears in these mutants. The signal detected for this new fragment, stronger than for KCT26/KCT20, suggests that the loss of the original conformation in this region modifies the residues that are accessible and/or in the right position for the action of the responsible protease(s), probably shifting the cleavage site. Alternatively, this new fragment could be the result of a new protease that can access a cleavage site hidden when the C6 domain is properly folded. However, the most obvious effect after alteration of the C6 domain either by mutagenesis or by deletion is the impairment of cleavage event 2, suggesting that a properly folded C6 domain is absolutely necessary for KIAA0319 to have the right conformation that allows proteolytic processing at site 2.

Detection of dimeric fragment KCT20 under non-reducing conditions in TM-Ct mutant (*OOM*) (Fig. 3*D*, *lane 4*) indicates that cleavage event 4 must occur N-terminal to the last Cys residue of the C6 domain (Cys-952). However, the KCT26/KCT20-like fragments from C6-deletion proteins

have similar sizes to those from C6 mutants despite the evidence that they must originate from cleavage at residues outside this domain. Therefore, it seems that the juxtamembrane ectodomain cleavage detected in the C6 mutant/deletion proteins is most probably heterogeneous, with no strict sequence specificity. This is not surprising as it has been described that in ADAM-mediated ectodomain shedding the cleavage sites are highly variable, and the secondary structure of the juxtamembrane stalk has critical importance for substrate recognition (20).

Ectodomain shedding is usually carried out by metalloproteases, in particular by members of the ADAM family (19, 22). However, other proteases have also been reported, the most significant being BACE1, also known as β-secretase, as its cleavage of APP at the β site initiates the production of amyloid β-peptide, critical in neurodegeneration in Alzheimer disease (32, 43). APP is not the only known substrate of BACE1; other proteins, such as neuregulin-1 or the cell adhesion protein P-selectin glycoprotein ligand-1, have been reported to be processed by this protease (43, 44). The proteases involved in ectodomain shedding of KIAA0319 have not been identified yet, and we are currently addressing this question. It is probable that the different cleavage events are carried out by different enzymes, and some preliminary results indicate that ADAMs are responsible for some of these events (data not shown).

From the functional point of view, the effect of the proteolytic cleavage of KIAA0319 is that the role of the full-length protein is terminated. Assuming that the function is cell adhesion, shedding of the ectodomain will eliminate the adhesive properties of this protein, and therefore, this could constitute a way for the cell to regulate the amount of full-length KIAA0319 protein at the plasma membrane. However, most of the proteolytic cleavage seems to occur after internalization from the plasma membrane as impairment of endocytosis drastically reduces the levels of C-terminal fragments. Therefore, our results here further support the importance of endocytosis in the regulation of the function(s) of KIAA0319 (16). Additionally, the relatively complex cleavage pattern of KIAA0319 is intriguing. If regulation of the potential adhesive role of this protein was the only function of its ectodomain shedding, only one or two of the detected cleavage events, namely events 3 and/or 4, would be required to accomplish that goal. However, cleavage event 1 occurs very close to the N terminus of the protein, and a small fragment containing the MANEC domain is released into the extracellular medium. The very little data known about the functional roles of the MANEC domain comes from studies on the hepatocyte growth factor activator inhibitor type 1 (HAI-1), a protein that also undergoes ectodomain shedding, where it is always referred to as "N-terminal domain" (45). It was proposed that this domain could be involved in the binding to the hepatocyte growth factor activator and to matriptase (13); however, recent deletion studies have shown that this domain does not bind specifically to matriptase but attenuates the inhibitory activity of HAI-1 by obstructing the protease binding sites (46). It is possible that release of the MANEC domain from KIAA0319 leads to a conformational and/or functional change of the protein; additionally, a signaling role of this domain cannot be ruled out. The rest of the cleavage events in the ectodomain of KIAA0319 would directly affect the adherent role of the protein either by disrupting the PKD region (event 2) or by releasing most of the ectodomain (events 3 and 4), providing they take place at the plasma membrane. Our results, however, suggest that processing at sites 2, 3, and 4 is favored after internalization from the plasma membrane, which indicates that this cleavage may be required for other reasons. One possibility is the regulation of the amount of KIAA0319 protein in the cell; after endocytosis from the plasma membrane, part of the molecules could be processed and destined for degradation, whereas others are redirected to the plasma membrane or to a subcellular compartment, such as the trans-Golgi network, that would act as an internal reservoir. Another option is that this ectodomain cleavage is required for signaling functions; cleavage event 5 (RIP) would be an essential component in this case. Intramembrane cleavage would free the remaining ectodomain stalk to the extracellular/luminal medium and the intracellular domain (KCT18) to the cytoplasm, and it is possible that both fragments have signaling roles. Fragments containing the C6 domain could be released to the extracellular medium by a combination of cleavage events, such as 2 + 5 or 3 + 5. The sequence of this domain ($CX_3CX_5CX_6CICX_{19}C$) resembles that of EGF-like modules (47, 48), in particular that of the cEGF subtype 1 module (49), although it is not recognized as such by the algorithms used in the databases for the different EGF-like motifs. EGF-like factors are synthesized as transmembrane precursors; the mature forms are released after ectodomain shedding and then bind to the ErbB cell surface receptors starting intracellular signal transduction cascades (48, 50). The EGF-like motifs are also present in many other proteins that are not growth factors, where their function could be to serve as structural spacers, although some of them can activate the EGF receptors (50). It could be possible that some of the released fragments of KIAA0319 containing the C6 domain trigger a signaling pathway after binding to a hypothetical receptor in a similar way as the EGF-like factors (26, 48). This could represent a new aspect in the functional characterization of the KIAA0319 protein to be considered in future analyses.

The ICDs of proteins that undergo RIP are released into the cytoplasm and, in this soluble form, can translocate to different compartments to carry out any associated biological activity (28). Because of the Notch model, ICDs are normally associated with nuclear translocation and regulation of gene expression after RIP, but only a few examples have actually been proven to work this way (33). Different subcellular compartments could be the final target of different ICDs, and the biological activity, if any, could be other than regulation of gene expression. These soluble fragments usually have a very short life, which makes their detection challenging, and therefore, overexpression experiments are normally used for their study. A very important point to be considered when interpreting experimental results concerning RIP is the stability of the cleaved products, although this is largely ignored by most investigators (37). The stability of a cytosolic protein is deter-

mined by the nature of its N-terminal residue, as the degradation of such proteins follow the "N-end rule" pathway (51, 52). Only a few amino acids are stabilizing residues (Met, Ala, Val, Ser, Thr, Pro, Gly), whereas the rest are destabilizing in different degrees and will trigger proteasomal degradation of the protein. Cys residues are considered destabilizing but only after oxidation, a process that necessitates the presence of a basic residue at position 2 of the substrate (thereby restricting this branch of the N-end rule pathway to a limited set of substrates) (51). An ICD that carries out a specific biological function after RIP would be expected to be stable enough to do so; in the absence of direct functional data, the first residue of the ICD could give an idea in this regard. Although we have not identified the exact cleavage point that releases the ICD of KIAA0319 (KCT18), our overexpression experiments suggest that the cleavage site is most probably located close to the C-terminal end of the TM domain; if we consider the C-terminal half of this domain, 7 of 12 amino acids would be stabilizing residues according to the N-end rule. We have analyzed the localization of several overexpressed KIAA0319 cytoplasmic domain fragments. In these experiments the overexpressed protein is artificially stabilized due to the initial Met residue; the amino acid at position 2 has to be taken into account as Met is removed by methionine aminopeptidase if this second residue has a small side chain (Cys, Ala, Val, Ser, Thr, Pro, Gly) and, therefore, the residue originally at position 2 would be the new N-terminal residue (51). All KCt constructs start with Met-Ala (Met-Val for EGFP-tagged proteins), so the encoded proteins are predicted to be stable. With these constructs we have shown that KCt can translocate to the nucleus and that it co-localizes with nucleoli. We could not detect nuclear localization of the C-terminal fragment originated after cleavage from the full-length protein. As mentioned above, detection of RIP fragments is often very challenging, and therefore, these results were not unexpected. The nuclear localization depends on the juxtamembrane region of this fragment, which contains an Arg/Lys-rich stretch of residues fitting the classical nuclear localization signal sequences (53). Despite the clear nuclear localization of the overexpressed KCt, there is no motif in this domain that could give an indication about its putative function, although this does not mean it has no biological activity. Even if KCt does localize to the nucleus in physiological conditions, it is very unlikely that it has any direct effect on gene expression; however, an indirect effect through interaction with transcription factors or other regulatory proteins could be possible. The subnuclear localization in nucleoli could support a putative indirect effect in gene regulation, maybe in a similar way as the nucleolar protein p14ARF regulates the activity of p53 in gene transcription (54).

The enzymes responsible for the cleavage of the KIAA0319 protein have not yet been identified. As mentioned above, those involved in its ectodomain shedding, that is, in cleavage events 1–4, could be a number of proteins from different families. On the other hand, the number of enzymes known to participate in intramembrane cleavage is much reduced, being γ-secretase the I-CLiP responsible in most of the type I proteins where RIP has been described. However, the fragments generated after this cleavage do not always have additional functions. This process could be just a disposal mechanism of membrane-tethered proteins/protein fragments, and it has been proposed that γ-secretase may function as "the proteasome of the membrane" (36, 37). We have addressed here the putative involvement of γ-secretase in KIAA0319 cleavage in different cell lines, including MEFs with no endogenous γ-secretase activity. Our results strongly suggest that γ-secretase is not involved in RIP of KIAA0319, and therefore, a different I-CLiP must be responsible for its intramembrane cleavage (event 5). The fact that KIAA0319 RIP is γ-secretase-independent could also suggest cleavage may have functional purposes other than the simple degradation of membrane-tethered KIAA0319 fragments and supports the hypothesis of a signaling function mentioned above. In future work identification of the proteases involved in the processing of KIAA0319 as well as the position of the different cleavage sites is necessary to understand the mechanisms behind this putative function.

Acknowledgments—We thank Prof. Bart DeStrooper (Center for Human Genetics, K. U. Leuven and VIB, Leuven, Belgium) for kindly providing MEF cells and Gal4-VP16 constructs and the Molecular Cytogenetics and Microscopy Core group for its technical support.

REFERENCES

1. Paracchini, S., Scerri, T., and Monaco, A. P. (2007) *Annu. Rev. Genomics Hum. Genet.* **8,** 57–79
2. Fisher, S. E., and Francks, C. (2006) *Trends Cogn. Sci.* **10,** 250–257
3. McGrath, L. M., Smith, S. D., and Pennington, B. F. (2006) *Trends Mol. Med.* **12,** 333–341
4. Galaburda, A. M., LoTurco, J., Ramus, F., Fitch, R. H., and Rosen, G. D. (2006) *Nat. Neurosci.* **9,** 1213–1217
5. Gabel, L. A., Gibson, C. J., Gruen, J. R., and LoTurco, J. J. (2010) *Neurobiol. Dis.* **38,** 173–180
6. Kidd, T., Brose, K., Mitchell, K. J., Fetter, R. D., Tessier-Lavigne, M., Goodman, C. S., and Tear, G. (1998) *Cell* **92,** 205–215
7. Andrews, W., Barber, M., Hernadez-Miranda, L. R., Xian, J., Rakic, S., Sundaresan, V., Rabbitts, T. H., Pannell, R., Rabbitts, P., Thompson, H., Erskine, L., Murakami, F., and Parnavelas, J. G. (2008) *Dev. Biol.* **313,** 648–658
8. Paracchini, S., Thomas, A., Castro, S., Lai, C., Paramasivam, M., Wang, Y., Keating, B. J., Taylor, J. M., Hacking, D. F., Scerri, T., Francks, C., Richardson, A. J., Wade-Martins, R., Stein, J. F., Knight, J. C., Copp, A. J., Loturco, J., and Monaco, A. P. (2006) *Hum. Mol. Genet.* **15,** 1659–1666
9. Dennis, M. Y., Paracchini, S., Scerri, T. S., Prokunina-Olsson, L., Knight, J. C., Wade-Martins, R., Coggill, P., Beck, S., Green, E. D., and Monaco, A. P. (2009) *PLoS Genet.* **5,** e1000436
10. Peschansky, V. J., Burbridge, T. J., Volz, A. J., Fiondella, C., Wissner-Gross, Z., Galaburda, A. M., Lo Turco, J. J., and Rosen, G. D. (2010) *Cereb. Cortex* **20,** 884–897
11. Velayos-Baeza, A., Toma, C., da Roza, S., Paracchini, S., and Monaco, A. P. (2007) *Mamm. Genome* **18,** 627–634
12. Velayos-Baeza, A., Toma, C., Paracchini, S., and Monaco, A. P. (2008) *Hum. Mol. Genet.* **17,** 859–871
13. Guo, J., Chen, S., Huang, C., Chen, L., Studholme, D. J., Zhao, S., and Yu, L. (2004) *Trends Biochem. Sci.* **29,** 172–174
14. Marchler-Bauer, A., Anderson, J. B., Chitsaz, F., Derbyshire, M. K., DeWeese-Scott, C., Fong, J. H., Geer, L. Y., Geer, R. C., Gonzales, N. R., Gwadz, M., He, S., Hurwitz, D. I., Jackson, J. D., Ke, Z., Lanczycki, C. J., Liebert, C. A., Liu, C., Lu, F., Lu, S., Marchler, G. H., Mullokandov, M., Song, J. S., Tasneem, A., Thanki, N., Yamashita, R. A., Zhang, D., Zhang, N., and Bryant, S. H. (2009) *Nucleic. Acids Res.* **37,** D205–D210

15. Ibraghimov-Beskrovnaya, O., Bukanov, N. O., Donohue, L. C., Dackowski, W. R., Klinger, K. W., and Landes, G. M. (2000) *Hum. Mol. Genet.* **9,** 1641–1649
16. Levecque, C., Velayos-Baeza, A., Holloway, Z. G., and Monaco, A. P. (2009) *Am. J. Physiol. Cell Physiol.* **297,** C160–C168
17. Reiss, K., Ludwig, A., and Saftig, P. (2006) *Pharmacol. Ther.* **111,** 985–1006
18. Stemmler, M. P. (2008) *Mol. Biosyst.* **4,** 835–850
19. Arribas, J., and Borroto, A. (2002) *Chem. Rev.* **102,** 4627–4638
20. Seals, D. F., and Courtneidge, S. A. (2003) *Genes Dev.* **17,** 7–30
21. Huovila, A. P., Turner, A. J., Pelto-Huikko, M., Kärkkäinen, I., and Ortiz, R. M. (2005) *Trends Biochem. Sci.* **30,** 413–422
22. Reiss, K., and Saftig, P. (2009) *Semin. Cell Dev. Biol.* **20,** 126–137
23. McCawley, L. J., and Matrisian, L. M. (2001) *Curr Opin Cell Biol.* **13,** 534–540
24. Blobel, C. P. (2005) *Nat. Rev. Mol. Cell Biol.* **6,** 32–43
25. Murphy, G. (2008) *Nat. Rev. Cancer* **8,** 929–941
26. Higashiyama, S., Iwabuki, H., Morimoto, C., Hieda, M., Inoue, H., and Matsushita, N. (2008) *Cancer Sci.* **99,** 214–220
27. Brown, M. S., Ye, J., Rawson, R. B., and Goldstein, J. L. (2000) *Cell* **100,** 391–398
28. Urban, S., and Freeman, M. (2002) *Curr. Opin. Genet. Dev.* **12,** 512–518
29. Weihofen, A., and Martoglio, B. (2003) *Trends Cell Biol.* **13,** 71–78
30. Beel, A. J., and Sanders, C. R. (2008) *Cell. Mol. Life Sci.* **65,** 1311–1334
31. Wolfe, M. S. (2009) *J. Biol. Chem.* **284,** 13969–13973
32. Annaert, W., and De Strooper, B. (2002) *Annu. Rev. Cell Dev. Biol.* **18,** 25–51
33. Wakabayashi, T., and De Strooper, B. (2008) *Physiology* **23,** 194–204
34. Tolia, A., and De Strooper, B. (2009) *Semin. Cell Dev. Biol.* **20,** 211–218
35. Selkoe, D., and Kopan, R. (2003) *Annu. Rev. Neurosci.* **26,** 565–597
36. Kopan, R., and Ilagan, M. X. (2004) *Nat. Rev. Mol. Cell Biol.* **5,** 499–504
37. Hass, M. R., Sato, C., Kopan, R., and Zhao, G. (2009) *Semin. Cell Dev. Biol.* **20,** 201–210
38. Herreman, A., Hartmann, D., Annaert, W., Saftig, P., Craessaerts, K., Serneels, L., Umans, L., Schrijvers, V., Checler, F., Vanderstichele, H., Baekelandt, V., Dressel, R., Cupers, P., Huylebroeck, D., Zwijsen, A., Van Leuven, F., and De Strooper, B. (1999) *Proc. Natl. Acad. Sci. U.S.A.* **96,** 11872–11877
39. Herreman, A., Van Gassen, G., Bentahir, M., Nyabi, O., Craessaerts, K., Mueller, U., Annaert, W., and De Strooper, B. (2003) *J. Cell Sci.* **116,** 1127–1136
40. Aricescu, A. R., Lu, W., and Jones, E. Y. (2006) *Acta Crystallogr. D Biol. Crystallogr.* **62,** 1243–1250
41. Serneels, L., Dejaegere, T., Craessaerts, K., Horré, K., Jorissen, E., Tousseyn, T., Hébert, S., Coolen, M., Martens, G., Zwijsen, A., Annaert, W., Hartmann, D., and De Strooper, B. (2005) *Proc. Natl. Acad. Sci. U.S.A.* **102,** 1719–1724
42. Tousseyn, T., Thathiah, A., Jorissen, E., Raemaekers, T., Konietzko, U., Reiss, K., Maes, E., Snellinx, A., Serneels, L., Nyabi, O., Annaert, W., Saftig, P., Hartmann, D., and De Strooper, B. (2009) *J. Biol. Chem.* **284,** 11738–11747
43. Stockley, J. H., and O'Neill, C. (2008) *Cell. Mol. Life Sci.* **65,** 3265–3289
44. Cole, S. L., and Vassar, R. (2008) *Curr. Alzheimer Res.* **5,** 100–120
45. Kataoka, H., Shimomura, T., Kawaguchi, T., Hamasuna, R., Itoh, H., Kitamura, N., Miyazawa, K., and Koono, M. (2000) *J. Biol. Chem.* **275,** 40453–40462
46. Kojima, K., Tsuzuki, S., Fushiki, T., and Inouye, K. (2008) *J. Biol. Chem.* **283,** 2478–2487
47. Campbell, I. D., and Bork, P. (1993) *Curr. Opin. Struct. Biol.* **3,** 385–392
48. Sanderson, M. P., Dempsey, P. J., and Dunbar, A. J. (2006) *Growth Factors* **24,** 121–136
49. Wouters, M. A., Rigoutsos, I., Chu, C. K., Feng, L. L., Sparrow, D. B., and Dunwoodie, S. L. (2005) *Protein Sci.* **14,** 1091–1103
50. Schneider, M. R., and Wolf, E. (2009) *J. Cell. Physiol.* **218,** 460–466
51. Mogk, A., Schmidt, R., and Bukau, B. (2007) *Trends Cell Biol.* **17,** 165–172
52. Tasaki, T., and Kwon, Y. T. (2007) *Trends Biochem. Sci.* **32,** 520–528
53. Lange, A., Mills, R. E., Lange, C. J., Stewart, M., Devine, S. E., and Corbett, A. H. (2007) *J. Biol. Chem.* **282,** 5101–5105
54. Boisvert, F. M., van Koningsbruggen, S., Navascués, J., and Lamond, A. I. (2007) *Nat. Rev. Mol. Cell Biol.* **8,** 574–585